Original Article
DOI: 10.22037/jds.v40i2.41031
ISSN 2645-4351

Anatomical Variations of the Greater Palatine Canal and Greater Palatine Foramen in an Iranian Subpopulation Using Cone-Beam Computed Tomography

Aisan Ghaznavi [a], **Maryam Mostafavi** [a], **Mandana Alamdari Mahd** [b]

[a]Assistant Professor, Dept. of Oral and Maxillofacial Radiology, School of Dentistry, Urmia University of Medical Sciences, Urmia, Iran.
[b]Postgraduate Student, Dept. of Pediatric Dentistry, School of Dentistry, Islamic Azad University of Tehran, Iran.
Correspondence to Mandana Alamdari Mahd (email: m.alamdari@student.iautmu.ac.ir).
(*Submitted: 31 January 2022 – Revised version received: 26 February 2023 – Accepted: 01 March 2023– Published online: Spring 2023*)

Objectives This study aimed to assess the anatomical variations of the greater palatine canal (GPC) and greater palatine foramen (GPF) in an Iranian subpopulation using cone-beam computed tomography (CBCT).
Methods This cross-sectional study was conducted on 193 CBCT scans of adults (94 males, 99 females) taken between 2017-2021 that were retrieved from a radiology clinic in Urmia, Iran. Axial sections were used to assess the position, diameter, and shape of GPF, and sagittal sections were used to assess the length and path of GPC. Data were analyzed by paired and independent t-test, Wilcoxon test, Mann-Whitney test, and Chi-square test (alpha=0.05).
Results In most cases (97.34% of males and 98.49% of females), GPF was located distal to the maxillary first molar. The mean distance between the GPF and midpalatal suture was significantly greater in males than females (15.2±1.8 vs. 14.3±1.5 mm; P=0.002). The mean diameter of GFP was significantly larger in males than females in both mesiodistal (2.34±0.64 vs. 1.96±0.63 mm, P<0.05) and anteroposterior (4.69±1.17 vs. 4.07±1.20 mm, P=0.001) dimensions. The mean length of GPC in males was significantly higher than that in females (28.55±2.62 vs. 26.90±3.31 mm, P<0.05). The most common form of GPF and GPC (on sagittal sections) was oval, and sigmoid, and curve, respectively. The most common GPC path was anterior-inferior (65.96% of males and 64.65% of females).
Conclusion The present results provided valuable information regarding the anatomical variations of GPF and GPC in Iranian population. CBCT was proven to be a valuable tool for assessment of maxillofacial anatomical landmarks.
Keywords Cone-Beam Computed Tomography; Maxillary Nerve; Anatomy; Greater Palatine Canal

Introduction

The greater palatine canal (GPC) is initiated from the inferior part of the pterygopalatine fossa (PPF) and extends to the hard palate. The GPC provides a straight access to the PPF, and contains important components including the pterygopalatine ganglion, maxillary nerve division of the trigeminal nerve and its branches (zygomatic nerve, superior-posterior alveolar nerve, and infraorbital nerve), pterygoid nerve, and distal branches of the maxillary artery, and veins. [1] The anatomy and position of the GPC are highly important for dental clinicians with regard to the procedures conducted in this region (such as anesthetic injection, implant placement, LeFort osteotomy, and sinonasal surgeries). [2]

Local anesthetic injection into the PPF through the GPC provides deep anesthesia in half of the maxillary teeth along with the adjacent soft and hard tissues, sinus, skin of the midface, and nasal cavity. [3] Thus, blocking of greater palatine nerve is suggested for several procedures, including surgical procedures of maxillary molars, maxillary sinus, and nasal cavity, control of posterior nasal bleeding, anesthesia of maxillary branch of trigeminal nerve, and treatment of sphenopalatine neuralgia. [4, 5] Blocking of the maxillary division of the trigeminal nerve and its branches is commonly performed to induce local anesthesia for oral and maxillofacial surgical procedures, which is conventionally performed intraorally through the greater palatine foramen (GPF) into the GPC. [6] However, nerve block anesthesia may fail due to difficult detection of greater palatine fossa. [4] This technique can have complications as well. Over-estimation or under-estimation of GPC length can cause inadequate anesthesia or its spread to the adjacent organs such as the orbit and nasal cavity and lead to diplopia, ptosis, permanent paresthesia, temporary ophthalmoplegia, permanent blindness, and unconsciousness. [7] The position of GPC is also important to prevent bleeding and anesthesia failure in palatal mucosa grafts in periodontal surgical procedures. Moreover, in implant treatment of maxillary molars, knowledge about the position of trabecular bone (maxillary tuberosity, pterygoid process of the sphenoid bone, and pyramidal process of the palatine bone) and the adjacent structures is imperative. GPC is among the most important structures in this region. [8] Assessment of anatomical dimensions and radiographic landmarks in the pterygomaxillary region such as the anatomical position of GPC and its distance from the adjacent structures is imperative prior to placement of pterygoid implants. [9]

In clinical examination, maxillary molars and mid-palatal suture are the most beneficial references for determination of the intraoral position of the GPF. GPF block is effective for induction of anesthesia and control of bleeding in paranasal sinus surgery. [10] Studies on dry human skulls revealed the position of GPF to be around the maxillary second and third molars. Limited studies have assessed the dimensions of GPF using computed tomography. [11, 12] Computed tomography and cone-beam computed

tomography (CBCT) enable precise assessment of the dimensions and position of the GPF relative to the maxillary molar and mid-palatal suture and allow measurement of the length of GPC based on gender and laterality. [4, 13]

Considering all the above, knowledge about the anatomical variations of the GPC and GPF is highly important for clinicians in different populations and can greatly help in safe and efficient administration of local anesthesia, implant placement, and conduction of LeFort I osteotomy and sinonasal surgeries. Accordingly, this study aimed to assess the anatomical variations of the GPC and GPF in an Iranian subpopulation residing in Urmia, Iran using CBCT.

Methods and Materials

This cross-sectional study was conducted on 193 maxillary CBCT scans (visualizing 386 GPCs) taken between 2017 to 2021, that were retrieved from the archives of a radiology clinic in Urmia, Iran. The study protocol was approved by the ethics committee of Urmia University of Medical Sciences (IR.UMSU.REC.1396.198).

The sample size was calculated to be 386 GPCs using the Cochrane formula assuming Z=1.96, 95% confidence interval, d=0.05, and P=0.05 [N=(ZS/d)2].

The inclusion criteria were (I) minimum age of 18 years, (II) CBCT scans taken with a voxel size of 0.3 mm or smaller, (III) bilateral presence of erupted maxillary molars, and (IV) absence of pathological conditions and jaw deformities.

The exclusion criteria were (I) history of trauma or orthognathic or craniofacial surgery, (II) presence of intrabony pathological lesions in the maxilla, (III) syndromic patients, (IV) absence of GPF, (V) ossification of GPC, (VI) presence of dental implants at the premolar or molar sites, and (VII) presence of artifacts at the site of interest.

All CBCT scans had been taken with Scanora 3D CBCT scanner (Soredex®, Helsinki, Finland) with 90 kVp, 12 mA, and 0.3 mm or smaller voxel size. All images were evaluated by two oral and maxillofacial radiologists with a minimum of 3 years of clinical experience using Romexis® 3.8.2 software. To standardize the observations and interpretations, the two observers were calibrated by reassessing 10% of all CBCT scans for the second time. The CBCT images were displayed on a 17-inch LG® monitor with 1024 x 1280 resolution and 32-bit color depth.

Axial sections were used to assess the position and dimensions of GPF, and sagittal sections were used to measure the GPC length.

(I) Position of GPF relative to the maxillary first molar: The position of GPF was identified by drawing a line perpendicular to the mid-palatal suture from the distal of first molar at the interdental area (Figures 1 and 2).

Figure 1: Line passing through the distal aspect of maxillary first molar perpendicular to the mid-palatal suture on the axial view

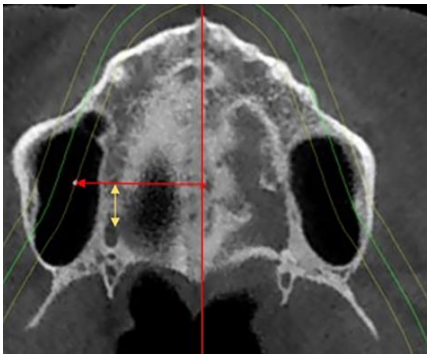

Figure 2: Position of GPF relative to the line passing through the distal of maxillary first molar perpendicular to the mid-alatal suture on the axial view

(II) Width (diameter) of GPF: It was measured antero-posteriorly (by connecting the most anterior and the most posterior points of the foramen) and horizontally (by connecting the most mesial and most distal points of the foramen).

(III)GPC length: The length and path of the canal were assessed on sagittal sections using the Haward-Swirzinski method. [13] Canal length was measured from the center of the pterygoid canal (as the center of PPF) to GPF at the inferior surface of the hard palate. The straightest path passing through the center of the canal was considered, and the GPC path on the sagittal section was assessed.

(IV) Shape of GPF and GPC: Since GPC opens into the hard palate through the GPF, a horizontal line was drawn in the inferior third of the GPC on the sagittal section, and the shape of GPF was assessed on axial section. On the sagittal section, the shape of the GPC was assessed at the level of the palate where the GPC is widened to form the PPF to the pterygopalatine canal. The axial shapes of the GPF included oval, teardrop, drop of water, banana, kidney, circular, smoke, triangle, crescent, diamond, and figure of eight. (Figure 3).

Different shapes of GPC on the sagittal section included waterfall, hourglass, curve, sigmoid, letter E, and straight (Figure 4).

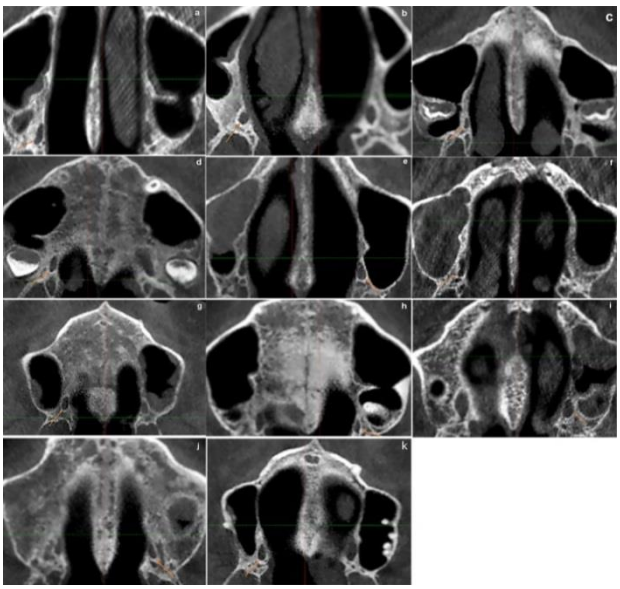

Figure 3: Different axial shapes of GFP: (a) triangle, (b) circle, (c) banana, (d) diamond, (e) drop of water, (f) figure of eight, (g) oval, (h) smoke, (i) kidney, (J) crescent, (k) teardrop.

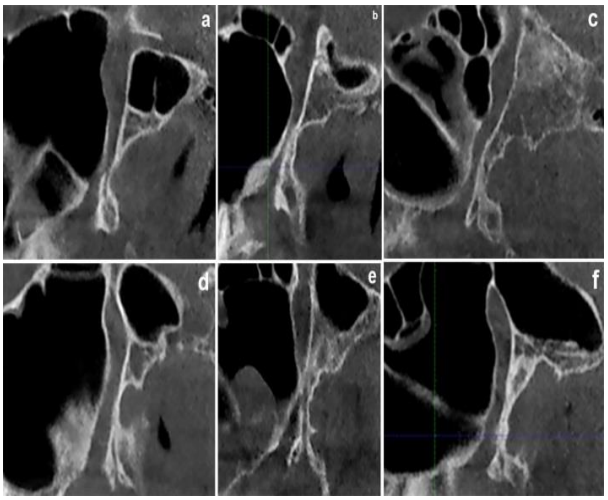

Figure 4: Sagittal classification of GPC shapes: (a) waterfall, (b) curve, (c) E shaped, (d) sigmoid, (e) hourglass, (f) straight.

Demographic information of patients including the age and gender was also extracted from the patient records. The right and left sides of each patient were evaluated.
Data were analyzed by SPSS version 19 using the Chi-square test at 0.05 level of significance.

Results

CBCT scans of a total of 193 patients were evaluated including 94 males (48.7%) and 99 females (51.3%). The intraclass correlation coefficient for the inter-observer agreement was found to be over 0.9.

Position of the GPF relative to the maxillary first molar in males and females:

GPF had a posterior position in 97.34% of males and 98.49% of females. It was on the line passing through the distal of maxillary first molar and perpendicular to the mid-palatal suture in 2.66% of males and 1.51% of females. The Wilcoxon test showed no significant difference in position of GPF between males and females (P=0.61).

Position of the GPF relative to the maxillary first molar at the right and left sides:

The position of GPF was posterior in 97.4% and on the line in 2.6% of the cases at the right side; these values were 98.4% and 1.6%, respectively, at the left side. The Wilcoxon test showed no significant difference in position of GPF between the right and left sides (P=0.157).

Distance from the GPF to the midpalatal suture based on gender:

Considering the normal distribution of data, independent t-test was applied which showed that the mean distance between the GPF and midpalatal suture was significantly greater in males than females in both the right and left sides (15.20±1.84 mm vs. 14.37±1.54 mm; P=0.002).

Distance from the GPF to the midpalatal suture at the right and left sides:

Considering the normal distribution of data, paired t-test was applied which showed no significant difference in this parameter between the right and left sides (14.94±1.74 mm in the right side vs. 14.61±1.73 mm in the left side, P=0.158).

Mesiodistal and anteroposterior diameter (width) of the GPF based on gender:

The Mann-Whitney test showed that the mean diameter of GPF was significantly greater in males than females in both mesiodistal (2.34±0.64 vs. 1.96±0.63 mm, P<0.05) and anteroposterior (4.69±1.17 vs. 4.07±1.20 mm, P=0.001) dimensions. The difference of mesiodistal or anteroposterior diameter of GPF between the right and left sides was not significant (P>0.05).

GPC length based on gender:

According to the Mann-Whitney test, the mean length of the GPC in males was significantly higher than that of females (28.55±2.62 vs. 26.90±3.31 mm, P<0.05).

GPC length at the right and left sides:

According to the Wilcoxon test, the mean length of the GPC at the right side was significantly greater than that of the left side (27.80±2.81 mm vs. 27.61±3.4 mm, P=0.012).

Shape of the GPF based on gender:

Table 1 presents the frequency distribution of different shapes of the GPF in males and females. As shown, oval shape had the highest frequency in males. In females, the diamond shape had the highest frequency followed by the oval shape. The difference in this regard was significant

between males and females (Chi-square test, P=0.001).

Table 1- Frequency distribution of different shapes of GPF in males and females

Gender	Males		Females	
GPF shape	Frequency	Percentage	Frequency	Percentage
Circle	23	12.23	35	17.68
Oval	77	40.95	38	19.18
Teardrop	10	5.32	10	5.05
Drop of water	14	7.45	13	6.57
Crescent	2	1.06	7	3.54
Diamond	14	7.45	40	20.2
Triangle	18	9.57	5	2.52
Smoke	4	2.13	7	3.54
Kidney	4	2.13	7	3.54
Figure 8	10	5.32	27	13.63
Banana	12	6.38	9	4.55
Right and left	188	100	198	100

Shape of the GPF at the right and left sides:

Table 2 presents the frequency distribution of different shapes of the GPF at the right and left sides. As shown, the oval shape had the highest frequency in both the right and left sides. The difference in this regard was not significant between the right and left sides (Chi-square test, P=0.178).

Table 2- Frequency distribution of different shapes of GPF in the right and left sides

Side	Right		Left	
GPF shape	Frequency	Percentage	Frequency	Percentage
Circle	26	13.5	32	16.6
Oval	66	34.1	49	25.3
Teardrop	11	5.7	9	4.7
Drop of water	8	4.1	19	9.8
Crescent	6	3.1	3	1.6
Diamond	28	14.5	26	13.4
Triangle	10	5.1	13	6.7
Smoke	6	3.1	5	2.5
Kidney	8	4.1	3	1.5
Figure 8	14	7.2	23	11.9
Banana	10	5.1	11	5.6
Right and left	193	100	193	100

Shape of the GPC based on gender:

Table 3 presents the frequency distribution of different shapes of the GPC in males and females. As shown, the sigmoid type had the highest frequency in males while the curve type had the highest frequency in females. The Chi-square test showed no significant difference in this regard between males and females (P=0.395).

Table 3- Frequency distribution of different shapes of GPC in males and females

Gender	Males		Females	
GPC shape	Frequency	Distribution	Frequency	Distribution
Waterfall	11	5.84	8	4.04
Curve	69	36.7	75	37.88
E	5	2.7	11	5.56
Sigmoid	80	42.54	72	36.36
Hourglass	2	1.06	5	2.53
Straight	21	11.16	27	13.63
Right and left	188	100	198	100

Shape of the GPC at the right and left sides:

Table 4 presents the frequency distribution of different shapes of the GPC in the right and left sides. As indicated, the curve shape had the highest frequency in the right side while the sigmoid shape had the highest frequency in the left side. According to the Chi-square test, the difference between the right and left sides was significant in this regard (P=0.005).

GPC path:

Table 5 presents the path of the GPC in males and females. As indicated, the anterior-inferior path had the highest

frequency in both males and females. The difference in this regard was not significant between males and females (Chi-square test, P=0.776).

Table 4- Frequency distribution of different shapes of GPC in the right and left sides

Side	Right		Left	
GPC shape	Frequency	Percentage	Frequency	Percentage
Waterfall	10	5.2	9	4.7
Curve	88	45.6	56	29
E	6	3.1	10	5.2
Sigmoid	59	30.6	93	48.2
Hourglass	3	1.6	4	2.1
Straight	27	14	21	10.9
Right and left	193	100	193	100

Table 5- Path of GPC in males and females

Gender	Males		Females	
GPC path	Frequency	Percentage	Frequency	Percentage
inf. direction	54	28.72	56	28.28
ant.inf	124	65.96	128	64.65
inf+ant.inf+inf	10	5.32	14	7.07
Right and left	188	100	198	100

Table 6 presents the path of GPC in the right and left sides. The difference in this regard was not significant between the right and left sides (Chi-square test, P=0.328).

Table 6- Path of GPC in the right and left sides

Side	Right		Left	
GPC path	Frequency	Percentage	Frequency	Percentage
inf. direction	49	25.4	61	31.6
ant.inf	130	67.3	122	63.2
inf+ant.inf+inf	14	7.3	10	5.2
Males and females	193	100	193	100

Discussion

This study assessed the anatomical variations of the GPC in an Iranian subpopulation residing in Urmia, Iran using CBCT. CBCT is extensively used for radiographic assessments of the head and neck region due to provision of high-resolution images. It is also commonly used for assessment of the morphology of maxillary and mandibular structures such as the nasopalatine canal, and position of the mandibular canal. [14] Another advantage of CBCT is that it helps to determine the age and gender of patients, and enables assessment of all six maxillary molars as a reference for determination of the position of GPF. [4]

The results showed that in most cases (97.34% of males and 98.49% of females), the GPF was located distal to the maxillary first molar. Consistent with this finding, the majority of previous studies reported distal position of the GPF relative to the first molar. Saralaya and Nayak [11] observed that the GPF was at the level of the maxillary first molar in 74.6% and between the maxillary second and third molars in 24.2% of the cases. Aoun et al. [15] reported that the GPF was at the level of third molar in 41.38%, distal to third molar in 29.31%, between the second and third molars in 27.59%, and at the level of second molar in 1.72%. Ikuta et al. [4] reported that the GPF was at the third molar site in 92% of the cases. According to Chrcanovic and Custódio [16] GPF was at the level of, or distal to maxillary third molar in 93.81% of the cases. In the present study, the position of GPF was not significantly different between the right and left sides. However, some others reported asymmetrical position of the GPF at the two sides. [15] Aoun et al. [15] attributed this asymmetry to occlusal problems such as impaction or displacement of canine and premolar teeth, which might cause asymmetry in molar position and arch length.

In the present study, the mean distance between the GPF and midpalatal suture was significantly greater in males than females (15.2±1.8 vs. 14.3±1.5 mm; P=0.002). This distance was 16 mm in a Turkish population [17], 14 mm in a Brazilian population (16), 14.8 mm (right side) and 15 mm (left side) in an Indian population [18], 15.4 mm in a Nigerian population and 14.7 mm (right side) and 14.6 mm (left side) in an Indian population. [6] In the present study, this distance was not significantly different between the right and left sides, which was in line with the findings of Ajmani [6] and Saralaya and Nayak. [11]

In the present study, the mean diameter of GFP was

significantly greater in males than females in mesiodistal dimension (2.34±0.64 vs. 1.96±0.63 mm, P<0.05). Ikuta et al. [4] reported that the mean mesiodistal diameter of GPF was 3.1 mm in a Brazilian population. This diameter was 3 mm in a study by Nimigean et al. [10] A review study on 25 articles reported the mean diameter of the GPF to be 2.9 mm in males and 2.8 mm in females. [19] Bahşi et al. [20] reported the mean diameter of GPF to be 3.08 mm in females and 3.52 mm in males. Considering the results, it appears that the mean mesiodistal GPF diameter in the present study population was smaller than that of other populations. Significantly larger mesiodistal diameter of GPF in males than females was in agreement with the results of Tomaszewska et al, [19] and Bahşi et al. [20] The mean mesiodistal diameter of GPF was not significantly different between the right and left sides in the present study, which was in line with the results of Nimigean et al. [10] Tomaszewska et al. [19] reported significantly larger GPF diameter at the right side than the left side in males, but this difference was not significant in females.

The mean anteroposterior diameter of GPF was also significantly greater in males than females in the present study (4.69±1.17 vs. 4.07±1.20 mm, P=0.001). The anteroposterior diameter of the GPF was 5.3 mm in a Greek population [21], 5.1 mm in a Polish population [22], 4.9 mm in a Thai population [12], 4.7 mm in an Indian population [23] and 4.5 mm in a Korean population. [24] In the present study, the mean anteroposterior GPF diameter was significantly larger in males than females, which was in line with the results of Aoun et al. [25] Also, a review study showed significantly larger mean anteroposterior GPF diameter in males (5.1 mm) than females (5 mm). The mean anteroposterior diameter of GPF in the present study was 4.41±1.20 mm at the right and 4.34±1.25 mm at the left side. These values were similar to those reported by Sharma and Garud [23] in an Indian population (4.67±1.13 in the right and 4.88±1.58 mm in the left side). Also, this value was 4.9±0.9 mm in the study by Nimigean et al. [10] However, the anteroposterior GPF diameter in the present study was smaller than the value reported by Aoun et al [25], (6.38±1.28 mm in the right side and 6.42±1.09 mm in the left side). In the present study, the mean anteroposterior GPF diameter was not significantly different between the right and left sides, which was in accordance with previous findings [10,19,25].

The mean length of the GPC in males was significantly greater than that of females (28.55±2.62 vs. 26.90±3.31 mm, P<0.05) in the current study. Sheikhi et al. [26] evaluated an Iranian population in Isfahan city and reported the mean length of the GPC to be 31.82±1.37 mm. Similar to the present findings, Das et al. [27] reported the GPC length to be 28±2 mm in males and 27±2 mm in females in the United States. This length was reported to be 29±3 mm in the United States [13], 29.7±4.2 mm in Thailand [12], and 31.1±2.9 mm in Poland. [19] The value obtained in the present study was much larger than the value reported by McKinney et al [5], that reported a length of 19.36±2.76 mm in adults. Also, Douglas and Wormald [28] reported this length to be 18.5 mm. It appears that the variations in the reported values can be due to differences in study populations or methodologies of studies. The present study revealed significantly greater length of the GPC in males than females, which was similar to the results of Sheikhi et al. [26] However, Aoun and Nasseh [3] reported no significant difference in GPC length between males and females. In the present study, GPC length was not significantly different between the right and left sides, which was similar to the findings of Sheikhi et al [26], and Aoun and Nasseh. [3] However, Valizadeh et al.[29] reported significantly greater GPC length in the right side than the left side in both males (with a mean age of 65.16 years) and females (with a mean age of 64.33 years).

In the present study, the most common shape of GPF was oval, although diamond shape was slightly more common than oval in females. Significant difference existed in the frequency of GPF shapes between males and females, although such difference was not observed between the right and left sides. Similarly, Sushobhana et al. [30] evaluated a North Indian population and reported that oval shape was the most common form with no significant difference between the right and left sides. Nimigean et al. [10] demonstrated that the oval shape was the most common shape in a southeast European population. Also, Methathrathip et al. [12] indicated the oval form to be the most common form in a Thai population. However, a review study by Tomaszewska et al. [22] reported that in some communities including central and South Africa, Nigeria, India, and Poland, GPF had an elongated form instead of oval.

In the present study, the most common forms of GPC on sagittal sections were sigmoid and curve. Although no significant difference existed between males and females in this regard, the difference between the right and left sides was significant, and curve form was more common in the right, and sigmoid form was more common in the left side. Studies on the form of GPC on sagittal sections are scarce. Rapado-González et al. [31] reported the most common GPC form on the sagittal sections to be hourglass (23.64%) in Spain.

In the present study, the most common GPC path was anterior-inferior (65.96% of males and 64.65% of females). Nimigean et al. [10] reported the frequency of anterior-inferior-medial path of GPC to be 82%. In a study by Howard-Swirzinski et al [13], the most common canal path on coronal sections was inferior-lateral followed by a straight downward path (43.3%). On the sagittal sections, anterior-inferior canal path was the most common pattern (92.9%).

The present study was conducted on an Iranian subpopulation. Further studies are required to assess the GPC and GPF in other subpopulations residing in other parts of Iran.

Conclusion

This study provided valuable information regarding the anatomical variations of GPC and GPF in an Iranian subpopulation residing in Urmia, Iran, that can greatly help the clinicians in conduction of surgical procedures in this region. GPF was located distal to the maxillary first molar in most cases. The mean distance from the GPF to the midpalatal suture was significantly greater in males than females. The mean diameter of the GPF was significantly greater in males than females in both mesiodistal and anteroposterior dimensions. The mean length of the GPC in males was significantly higher than that of females. The most common form of GPF was oval, and the most common forms of GPC on sagittal sections were sigmoid and curve. The most common GPC path was anterior-inferior.

Conflict of Interest

No Conflict of Interest Declared ■

References

1. Tashi S, Purohit BS, Becker M, Mundada P. The pterygopalatine fossa: imaging anatomy, communications, and pathology revisited. Insights. Imaging 2016;7:589-99.
2. Asha ML, Arun Kumar G, Sattigeri Anupama V, Raja Jigna V, Diksha M. Cone beam computed tomographic analysis of anatomical variations of greater palatine canal and foramen in relation to gender in South Indian population. Oral Health Dent Manag 2015;14:384-90.
3. Aoun G, Nasseh I. The Length of the Greater Palatine Canal in a Lebanese Population: a Radio-anatomical Study. Acta Inform Med 2016;24:397-400.
4. Ikuta CR, Cardoso CL, Ferreira-Júnior O, Lauris JR, Souza PH, Rubira-Bullen IR. Position of the greater palatine foramen: an anatomical study through cone beam computed tomography images. Surg Radiol Anat 2013;35:837-42.
5. McKinney KA, Stadler ME, Wong YT, Shah RN, Rose AS, Zdanski CJ, et al. Transpalatal greater palatine canal injection: Radioanatomic analysis of where to bend the needle for pediatric sinus surgery. Am J Rhinol Allergy 2010;24:385-8.
6. Ajmani ML. Anatomical variation in position of the greater palatine foramen in the adult human skull. J Anat 1994;184:635-7.
7. Suzuki M, Omine Y, Shimoo Y, Yamamoto M, Kaketa A, Kasahara M, et al. Regional Anatomical Observation of Morphology of Greater Palatine Canal and Surrounding Structures. Bull Tokyo Dent Coll 2016;57:223-31.
8. Uchida Y, Yamashita Y, Danjo A, Shibata K, Kuraoka A. Computed tomography and anatomical measurements of critical sites for endosseous implants in the pterygomaxillary region: a cadaveric study. Int J Oral Maxillofac Surg 2017;46:798-804.
9. Dalili Z, Mahjoub P, Sigaroudi AK. Comparison between cone beam computed tomography and panoramic radiography in the assessment of the relationship between the mandibular canal and impacted class C mandibular third molars. Dent Res J (Isfahan) 2011;8:203-10.
10. Nimigean V, Nimigean VR, Buţincu L, Sălăvăstru DI, Podoleanu L. Anatomical and clinical considerations regarding the greater palatine foramen. Rom J Morphol Embryol 2013;54:779-83.
11. Saralaya V, Nayak SR. The relative position of the greater palatine foramen in dry Indian skulls. Singapore Med J 2007;48:1143-6.
12. Methathrathip D, Apinhasmit W, Chompoopong S, Lertsirithong A, Ariyawatkul T, Sangvichien S. Anatomy of greater palatine foramen and canal and pterygopalatine fossa in Thais: considerations for maxillary nerve block. Surg Radiol Anat 2005;27:511-6.
13. Howard-Swirzinski K, Edwards PC, Saini TS, Norton NS. Length and geometric patterns of the greater palatine canal observed in cone beam computed tomography. Int J Dent 2010;2010:292753.
14. Safi Y, Moshfeghi M, Rahimian S, Kheirkhahi M, Manouchehri ME. Assessment of nasopalatine canal anatomic variations using cone beam computed tomography in a group of Iranian population Iran J Radiol. 2017;14(1): e13480.
15. Aoun G, Nasseh I, Sokhn S, Saadeh M. Analysis of the greater palatine foramen in a Lebanese population using cone-beam computed tomography technology. J Int Soc Prev Community Dent 2015;5:S82-8.
16. Chrcanovic BR, Custódio AL. Anatomical variation in the position of the greater palatine foramen. J Oral Sci 2010;52:109-13.
17. Cagimni P, Govsa F, Ozer MA, Kazak Z. Computerized analysis of the greater palatine foramen to gain the palatine neurovascular bundle during palatal surgery. Surg Radiol Anat 2017;39:177-84.
18. Westmoreland EE, Blanton PL. An analysis of the variations in position of the greater palatine foramen in the adult human skull. Anat Rec 1982;204:383-8.
19. Tomaszewska IM, Kmiotek EK, Pena IZ, Średniawa M, Czyżowska K, Chrzan R, et al. Computed tomography morphometric analysis of the greater palatine canal: a study of 1,500 head CT scans and a systematic review of literature. Anat Sci Int 2015;90:287-97.
20. Bahşi İ, Orhan M, Kervancıoğlu P, Yalçın ED. Morphometric evaluation and clinical implications of the greater palatine foramen, greater palatine canal and pterygopalatine fossa on CBCT images and review of literature. Surg Radiol Anat 2019;41:551-67.
21. Piagkou M, Xanthos T, Anagnostopoulou S, Demesticha T, Kotsiomitis E, Piagkos G, et al. Anatomical variation and morphology in the position of the palatine foramina in adult human skulls from Greece. J Craniomaxillofac Surg 2012;40:e206-10.
22. Tomaszewska IM, Tomaszewski KA, Kmiotek EK, Pena IZ, Urbanik A, Nowakowski M, et al. Anatomical landmarks for the localization of the greater palatine foramen--a study of 1200 head CTs, 150 dry skulls, systematic review of literature and meta-analysis. J Anat 2014;225:419-35.
23. Sharma NA, Garud RS. Greater palatine foramen--key to successful hemimaxillary anaesthesia: a morphometric study and report of a rare aberration. Singapore Med J 2013;54:152-9.
24. Hwang SH, Seo JH, Joo YH, Kim BG, Cho JH, Kang JM. An anatomic study using three-dimensional reconstruction for

pterygopalatine fossa infiltration via the greater palatine canal. Clin Anat 2011;24:576-82.
25. Aoun G, Nasseh I, Sokhn S. Radio-anatomical Study of the Greater Palatine Canal and the Pterygopalatine Fossa in a Lebanese Population: A Consideration for Maxillary Nerve Block. J Clin Imaging Sci 2016;6:35.
26. Sheikhi M, Zamaninaser A, Jalalian F. Length and anatomic routes of the greater palatine canal as observed by cone beam computed tomography. Dent Res J (Isfahan) 2013;10:155-61.
27. Das S, Kim D, Cannon TY, Ebert CS Jr, Senior BA. High-resolution computed tomography analysis of the greater palatine canal. Am J Rhinol 2006;20:603-8.
28. Douglas R, Wormald PJ. Pterygopalatine fossa infiltration through the greater palatine foramen: where to bend the needle. Laryngoscope 2006;116:1255-7.
29. Valizadeh S, Ahmadi SM, Ahsaie MG, Vasegh Z, Jamalzadeh N. The Anatomical Position and Size of Greater Palatine Foramen and Canal in an Iranian Sample Using Cone Beam Computed Tomography. J Long Term Eff Med Implants 2022;32:73-80.
30. SuShobhAnA SR, Singh S, jigyASA PASSey RS, SinhA P. Anatomical study and clinical considerations of greater palatine foramen in adult human skulls of north Indian population. Int J Anat Radiol Surg 2015;4:41-6.
31. Rapado-González O, Suárez-Quintanilla JA, Suárez-Cunqueiro MM. Anatomical variations of the greater palatine canal in cone-beam computed tomography. Surg Radiol Anat 2017;39:717-3.

How to cite:
Ghaznavi A, Mostafavi M, Alamdari Mahd M. Anatomical Variations of the Greater Palatine Canal and Greater Palatine Foramen in an Iranian Subpopulation Using Cone-Beam Computed Tomography. J Dent Sch 2022;40(2):59-66.